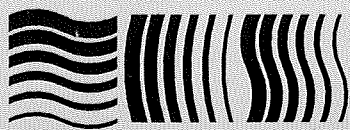


Dosimetry of low and medium energy x-rays

A code of practice for use in radiotherapy and radiobiology

NEDERLANDSE COMMISSIE VOOR STRALINGSDOSIMETRIE

Report 10 of the Netherlands Commission on Radiation Dosimetry



**Netherlands Commission on Radiation Dosimetry
Task Group Uniformity Dosimetry Protocols
July 1997**

Dosimetry of low and medium energy x-rays

A code of practice for use in radiotherapy and radiobiology

NEDERLANDSE COMMISSIE VOOR STRALINGSDOSIMETRIE

Report 10 of the Netherlands Commission on Radiation Dosimetry

Authors:

T.W.M. Grimbergen

A.H.L. Aalbers

B.J. Mijnheer

J. Seuntjens

H. Thierens

J. Van Dam

F.W. Wittkämper

J. Zoetelief

Netherlands Commission on Radiation Dosimetry

Task Group Uniformity Dosimetry Protocols

July 1997

Preface

The Nederlandse Commissie voor Stralingsdosimetrie (NCS, Netherlands Commission on Radiation Dosimetry) was officially established on 3 September 1982 with the aim of promoting the appropriate use of dosimetry of ionizing radiation both for scientific research and practical applications. The NCS is chaired by a board of scientists, installed upon the suggestion of the supporting societies, including the Nederlandse Vereniging voor Radiotherapie en Oncologie (Netherlands Society for Radiotherapy and Oncology), the Nederlandse Vereniging voor Klinische Fysica (Netherlands Society for Clinical Physics), the Nederlandse Vereniging voor Radiobiologie (Netherlands Society for Radiobiology), the Nederlandse Vereniging voor Stralingshygiëne (Netherlands Society for Radiological Protection), the Nederlandse Vereniging voor Biofysica (Netherlands Society for Biophysics), the Nederlandse Vereniging van Radiologisch Laboranten (Netherlands Society of Radiographers and Radiological Technologists) and the Ministry of Health, Welfare and Sports.

To pursue its aims the NCS accomplishes the following tasks: participation in dosimetry standardisation and promotion of dosimetry intercomparisons, drafting of dosimetry protocols, collection and evaluation of physical data related to dosimetry. Furthermore the commission shall maintain or establish links with national and international organisations concerned with ionizing radiation and promulgate information on new developments in the field of radiation dosimetry.

Current members of the board of the NCS:

J.J. Broerse, chairman

W. de Vries, secretary

J. Zoetelief, treasurer

A.J.J. Bos

R.B. Keus

W.C.A.M. Buijs

J.L.M. Venselaar

F.W. Wittkämper

D. Zweers

Dosimetry of low and medium energy x-rays
A code of practice for use in radiotherapy and radiobiology

Prepared by the task group Uniformity Dosimetry Protocols of the Netherlands Commission on Radiation Dosimetry (NCS) in cooperation with representatives of the Belgian Hospital Physicists Society (SBPH/BVZF), the University of Ghent (Belgium) and the Nederlands Meetinstituut (NMI). The authors wish to thank Dr. A.E. Nahum of the Institute of Cancer Research and Royal Marsden NHS Trust, Sutton (United Kingdom), for carefully reading the manuscript and providing valuable comments.

Members of the task group:

T.W.M. Grimbergen, chairman
A.H.L. Aalbers
J. Van Dam
B.J. Mijnheer
J. Seuntjens
H. Thierens
F.W. Wittkämper
J. Zoetelief

For further copies of this report or other NCS-reports see last page.

CONTENTS

| | |
|---|----|
| Summary of the recommendations | 1 |
| 1. Introduction | 2 |
| 1.1 <i>Scope</i> | 2 |
| 1.2 <i>Dosimetry of low and medium energy x-rays</i> | 3 |
| 1.3 <i>Basic equations for absorbed dose determination of low energy x-rays</i> | 4 |
| 1.4 <i>Basic equations for absorbed dose determination of medium energy x-rays</i> | 5 |
| 2. Code of practice for low energy x-rays (50-100 kV) | 8 |
| 2.1 <i>Reference chambers</i> | 8 |
| 2.2 <i>Calibration procedure</i> | 8 |
| 2.3 <i>Beam quality specification</i> | 8 |
| 2.4 <i>Reference conditions</i> | 8 |
| 2.5 <i>Determination of absorbed dose to water at the reference point</i> | 8 |
| 2.6 <i>Absorbed dose at other positions in the phantom</i> | 9 |
| 3. Code of practice for medium energy x-rays (100-300 kV) | 10 |
| 3.1 <i>Reference chamber</i> | 10 |
| 3.2 <i>Calibration procedure</i> | 10 |
| 3.3 <i>Beam quality specification</i> | 10 |
| 3.4 <i>Reference conditions</i> | 10 |
| 3.5 <i>Determination of absorbed dose to water</i> | 10 |
| 3.6 <i>Phantom materials</i> | 11 |
| 3.7 <i>Absorbed dose at other positions in the phantom</i> | 11 |
| 4. Additional information | 12 |
| 4.1 <i>General comments on low and medium energy x-ray dosimetry</i> | 12 |
| 4.2 <i>Comments on the code of practice for low energy x-rays</i> | 14 |
| 4.3 <i>Comments on the code of practice for medium energy x-rays</i> | 17 |
| 4.4 <i>Detectors to be used for relative dosimetry of low and medium energy x-rays</i> | 22 |
| 5. References | 23 |
| APPENDIX: Numerical values | 26 |

Summary of the recommendations

This report recommends the use of different formalisms for absorbed dose determination in two photon energy regions of interest in radiotherapy and radiobiology, *i.e.*: x-rays generated at tube voltages in the range 50-100 kV (low energy x-rays), and x-rays generated at tube voltages in the range 100-300 kV (medium energy x-rays). Equations are given to convert ionization chamber signal into absorbed dose to water for this type of radiation.

For low energy x-rays, the quantity to be determined under reference conditions is the photon absorbed dose to water at the surface of a water phantom. This quantity shall be determined from measurement of air kerma free-in-air (in the absence of the phantom) and application of appropriate conversion factors. The use of one of the reference ionization chambers is recommended. For absorbed dose determinations at other positions in the phantom (percentage depth doses or isodose curves) it is advised to use published data and/or information provided by the manufacturer of the x-ray equipment.

For medium energy x-rays, the quantity to be determined under reference conditions is the absorbed dose to water at the reference depth (2 cm). The absorbed dose shall be determined in a water phantom at the reference depth using the NE2571 chamber. Absorbed dose at other positions in the phantom shall be obtained by performing relative measurements with a field instrument and can be related to the value determined at the reference point.

The reference chamber shall be calibrated in air in terms of air kerma at the Primary Standard Dosimetry Laboratory in a beam of x-rays. The quality of the calibration field shall be as close as possible to that of the user's primary beam.

The data and procedures as presented in this report cover a broad range of radiation qualities, depths and field sizes. The use of this consistent set of data is strongly recommended.

1. Introduction

1.1 Scope

The present report fits into a series of NCS-reports on dosimetry of radiation beams used in radiotherapy. In previous reports, codes of practice for the dosimetry of high-energy photon beams [1], high-energy electron beams [2] and radioactive sources used in brachytherapy [3] were presented. This report deals with the dosimetry of low and medium energy x-rays.

From the results of questionnaires, distributed among radiotherapy centres, institutions for radiobiology and departments for diagnostic radiology in the Netherlands and Belgium, it appeared that the dosimetry in radiotherapy and radiobiology is quite different from that in diagnostic radiology. In diagnostic radiology, different beam qualities are used, other quantities (such as organ dose and effective dose) are of interest and the uncertainties allowed are larger. Therefore, it was decided to exclude the dosimetry of x-ray beams applied in diagnostic radiology from this report. Patient dosimetry in mammography has been presented in an earlier NCS-report [4]. Recently, a subcommittee on dosimetry in diagnostic radiology has been installed by the NCS board.

The results of the questionnaires received from the radiotherapy centres in the Netherlands and Belgium showed that, although the number of patients which are treated using low or medium energy x-rays is limited, almost all radiotherapy centres still apply these radiation qualities in practice to date. As old therapy machines are still being replaced by new ones, it is anticipated that the present practice will be continued in the future.

The need for a NCS-report on dosimetry of low and medium energy x-rays became evident from the replies on the questionnaires received from the radiotherapy centres and the institutions for radiobiology. A wide variety of beam qualities is in use, with generating potentials ranging from 50 kV up to 300 kV. A number of dosimetry protocols is applied, *i.e.* ICRU Report 17 [5], ICRU Report 23 [6] and "in-house" protocols. From the answers to the questionnaires it was concluded that, in addition to existing protocols, there was a need for recommendations to arrive at a more uniform approach.

In this report formalisms for dosimetry as well as a consistent set of data are presented, which under reference conditions (radiation quality, field size and depth in-phantom) yield absorbed dose values in agreement with updated information provided by the IAEA [7]. In addition, the procedures and data cover a broader range of radiation qualities, depths and field sizes than those given in the International Code of Practice of the IAEA [8], and are presented in a way that can be easily applied in practice.

Similar to the IAEA code of practice, the present report recommends the use of different formalisms in two photon energy regions of interest, *i.e.*: x-rays generated at tube voltages in the range 50-100 kV

(low energy x-rays), and x-rays generated at tube voltages in the range 100-300 kV (medium energy x-rays). The NCS code of practice resembles in this respect the recent IPEMB code of practice [9] for the determination of absorbed dose for x-rays below 300 kV generating potential, although the selected photon energy regions cover somewhat different radiation qualities. Also, most of our recommended sets of data are in agreement with the numerical data provided in the IPEMB code of practice. Unlike the present document, the IPEMB code also provides information on the determination of absorbed dose for very low energy x-rays, *i.e.* generated at tube voltages in the range 8-50 kV.

The underlying physics for the formalisms for low and medium energy x-rays is explained in the next sections. The actual codes of practice for low and medium energy x-rays are given in chapters 2 and 3, respectively. Chapter 4 provides additional background information, such as comments on detectors to be used for relative dosimetry. Finally, in the appendix tables are given with numerical values to be used in the code of practice.

1.2 *Dosimetry of low and medium energy x-rays*

The formalisms for absorbed dose determination in low and medium energy x-ray beams differ fundamentally from the method used for high energy photons. In the codes of practice for high energy photon beams, the Bragg-Gray cavity theory is applied to derive the absorbed dose to the medium from the absorbed dose to the ionization chamber gas using mass collision stopping power ratios averaged over the electron fluence spectrum at the chamber wall. To understand the basic principles of low and medium energy photon dosimetry the following aspects must be considered.

- (1) One of the basic assumptions of Bragg-Gray cavity theory, underpinning all present protocols for ionization chamber dosimetry of high energy photon and electron beams, is that the fluence and energy distributions of the secondary electrons at the chamber wall and in the air cavity are equal. This assumption is not valid for low and medium energy photons [10].
- (2) Bremsstrahlung production in water or air is negligible in this energy range, and therefore there is no practical difference between (total) kerma, K , and collision kerma, K_c .
- (3) Transient charged particle equilibrium is very easily established due to the small range of the electrons in water. As a consequence, absorbed dose to water, D_w , can, to a high degree of accuracy, be approximated by water collision kerma, $K_{c,w}$.

The latter two statements can be summarized as:

$$D_w = K_{c,w} = K_w \quad (1)$$

- (4) A feature specific to low and medium energy x-rays is that the proportion of scattered photons

relative to primary radiation present in a water phantom is much higher in this energy range compared with the situation for high energy photons. This has as a consequence that all correction and conversion coefficients have to be provided as a function of field size and depth in-phantom.

The next two sections explain the details of the principles underlying the procedures for absorbed dose determination in beams of low and medium energy x-rays. Equations are presented which allow to convert the ionization chamber signal into absorbed dose to water for this type of radiation. From the previous arguments it can be concluded that, in this energy region, the ionization chamber is considered to be a *kerma detector*. Secondary electrons, created outside the chamber wall do not have sufficient energy to contribute to the ionization in the cavity. It is therefore assumed that the chamber acts as a 'photon only' detector.

1.3 Basic equations for absorbed dose determination of low energy x-rays

For the deduction of the basic formula for absorbed dose determination in low energy x-rays, the formulation by Nahum and Knight [11] is followed. This procedure starts with a measurement of the kerma free-in-air with a calibrated ionization chamber and results in water kerma at the surface of a phantom which is assumed to represent absorbed dose at the surface.

The measurement with the calibrated chamber at the position of the entrance surface of the phantom (in absence of the phantom) gives the air kerma free-in-air, $K_{\text{air}}^{\text{free air}}$:

$$K_{\text{air}}^{\text{free air}} = M_u^{\text{free air}} N_K \quad (2)$$

where $M_u^{\text{free air}}$ is the corrected ionization chamber reading in the user's beam free-in-air (see paragraph 2.5 for a more extensive definition of $M_u^{\text{free air}}$) and N_K is the air kerma calibration factor for the beam quality concerned. The measured air kerma should then be converted to water kerma, which is effectively equal to absorbed dose to water in this energy range because of the small range of the secondary electrons. This can be done by using average mass energy absorption coefficient ratios water to air, $(\bar{\mu}_{\text{en}}/\rho)_{\text{w/air}}^{\text{free air}}$. Formally these ratios are calculated as:

$$(\bar{\mu}_{\text{en}}/\rho)_{\text{w/air}}^{\text{free air}} = \frac{\int_0^{E_{\text{max}}} (\mu_{\text{en}}(E)/\rho)_{\text{w}} E (d\Phi/dE)^{\text{free air}} dE}{\int_0^{E_{\text{max}}} (\mu_{\text{en}}(E)/\rho)_{\text{air}} E (d\Phi/dE)^{\text{free air}} dE} \quad (3)$$

where $(d\Phi/dE)^{\text{free air}}$ represents the photon fluence spectrum, differential in energy, E , of the primary x-ray beam free-in-air. Therefore, this ratio has no field size or depth dependence. The conversion of air kerma to water kerma, both free-in-air, is given by:

$$K_w^{\text{free air}} = K_{\text{air}}^{\text{free air}} (\bar{\mu}_{\text{en}}/\rho)_{w/\text{air}}^{\text{free air}} \quad (4)$$

Physically, $K_w^{\text{free air}}$ represents water kerma to a mass of water, small enough not to alter the primary photon fluence. The influence of the phantom is taken into account by introducing the backscatter factor B_w , which converts water kerma free-in-air into water kerma on the surface of a semi-infinite water phantom, thus defining the backscatter factor as a ratio of water kerma values (for a detailed discussion of definitions of the backscatter factor, see Grosswendt [12]):

$$K_w = K_w^{\text{free air}} B_w \quad (5)$$

It is important to realize that the dependence of the absorbed dose determination on field size and source-surface distance (SSD) is introduced by the backscatter factor. Finally, the absorbed dose at the phantom surface can be obtained by combining equations (1), (2), (4) and (5):

$$D_w = M_u^{\text{free air}} N_K B_w (\bar{\mu}_{\text{en}}/\rho)_{w/\text{air}}^{\text{free air}} \quad (6)$$

It should be born in mind that by using equation (1), it is assumed that there is transient charged particle equilibrium at the phantom surface. However, even for low energy photons, transient charged particle equilibrium is only present at a specific (small) depth in the phantom. This means that the absorbed dose at the surface defined by equation (6) in fact represents the absorbed dose at the minimum depth at which transient charged particle equilibrium is achieved, neglecting the photon attenuation over this depth. The actual dose at the surface is neither measurable nor clinically relevant and can be strongly affected by electron contamination present in the beam [13].

1.4 Basic equations for absorbed dose determination of medium energy x-rays

In contrast to the approach followed for low energy x-rays, for medium energy x-rays an ionization chamber is considered at a specific depth, d , in a phantom irradiated with a reference field. The chamber is calibrated free-in-air in terms of air kerma for a given x-radiation quality, with the same HVL and generating potential as the quality used for the irradiation of the phantom. Any deviations of the spectrum of the x-ray quality used for calibration and the spectrum used for the irradiation of the phantom, leading to a difference in the calibration factor N_K , are neglected.

The chamber measures kerma in the phantom, but the photon spectrum at the point of measurement is different from the spectrum free-in-air at which the chamber is calibrated, both regarding energy and angular distribution. Therefore a correction factor, k_{Q} , is introduced, which accounts for the change in calibration factor caused by this effect. Essentially a determination of this correction factor involves a study of the photon energy response as well as a study of the angular response of the chamber.

It is impractical to include the stem in the analysis of the angular response. The effect of photon scattering and attenuation caused by the presence of the chamber stem influences the calibration as well as the measurement in a phantom. The effect of change in calibration factor free-in-air, caused by the presence of the chamber stem, is accounted for by an additional factor k_{st} and its effect in-phantom by a factor p_{st} . By inserting the chamber into the phantom, the correct value of air-kerma in the cavity in the phantom, K_{air}^{cavity} can be measured, thus taking into account the stem effects and the change in response when photons come from all directions. Therefore:

$$K_{air}^{cavity} = M_u^d N_K k_\alpha k_{st} p_{st} \quad (7)$$

where M_u^d is the corrected ionization chamber reading in the user's beam, at depth d in the water phantom (see paragraph 3.5 for a more complete definition of M_u^d).

However, whereas the product $k_\alpha k_{st} p_{st}$ corrects the chamber response for differences in angular and energy distribution of the photons at the point of measurement and for the presence of the stem, it does not correct for the fact that, by inserting the chamber in the phantom, an amount of water material is displaced by the chamber. The volume of the water material displaced is determined by the chamber's outer dimensions. Therefore an additional correction factor, p_{disp} , is introduced which accounts for this effect. This factor should be considered as a correction factor for the change in air-kerma at the point of measurement due to the displacement of water [14]. Hence, the air kerma in the phantom at the point of measurement (without the chamber present) is given by:

$$K_{air} = K_{air}^{cavity} p_{disp} = M_u^d N_K k_\alpha k_{st} p_{st} p_{disp} \quad (8)$$

The measured air kerma is now converted into water kerma by using average mass energy absorption coefficient ratios. These ratios are calculated as:

$$\left(\bar{\mu}_{en}/\rho\right)_{w/air}^d = \frac{\int_0^{E_{max}} (\mu_{en}(E)/\rho)_w E (d\Phi/dE)^d dE}{\int_0^{E_{max}} (\mu_{en}(E)/\rho)_{air} E (d\Phi/dE)^d dE} \quad (9)$$

where $(d\Phi/dE)^d$ represents the photon fluence spectrum, differential in energy, at the point of measurement in the phantom. This spectrum can be derived from the primary photon fluence spectrum by Monte-Carlo calculations of photon transport in water. The resulting water kerma is given by:

$$K_w = K_{air} \left(\bar{\mu}_{en}/\rho\right)_{w/air}^d = M_u^d N_K k_\alpha k_{st} p_{st} p_{disp} \left(\bar{\mu}_{en}/\rho\right)_{w/air}^d \quad (10)$$

or, by applying equation (1):

$$D_w = K_w = M_u^d N_K k_\alpha k_{st} p_{st} p_{disp} (\bar{\mu}_{en}/\rho)_{w/air}^d \quad (11)$$

If the overall chamber correction factor, k_{ch} , is defined as:

$$k_{ch} = k_\alpha k_{st} p_{st} p_{disp} \quad (12)$$

the equation for absorbed dose to water proposed in this code of practice is obtained:

$$D_w = M_u^d N_K (\bar{\mu}_{en}/\rho)_{w/air}^d k_{ch} \quad (13)$$

By definition (12), the overall chamber correction factor has the same physical meaning as the correction factor k_{ch} used in the IPEMB code of practice [9]. In the revised formalism of the IAEA [7], the overall correction factor $k_{a,w}$ is introduced. This factor resembles k_{ch} but it includes in addition a correction factor for the effect of non-water equivalence of the waterproof sheath needed for non-watertight ionization chambers and a correction factor which accounts for any unknown effects (taken as unity). Additional information about the effect of the waterproof sheath is given in section 4.3.4.

Due to its definition, the overall chamber correction factor k_{ch} carries any chamber dependence in the correction procedure, whereas $(\bar{\mu}_{en}/\rho)_{w/air}^d$ is a chamber-independent conversion factor. However, it should be remembered that both factors are field size and depth dependent. Although the present code of practice addresses reference field size and reference depth (10 cm × 10 cm and 2 cm, respectively), more information on depth and field size dependence has been provided in sections 4.3.5 and 4.3.6. The code of practice recommends the use of a reference ionization chamber for which the relevant correction factors are known.

2. Code of practice for low energy x-rays (50-100 kV)

- 2.1 *Reference chambers:* The absorbed dose to water at the reference point shall be determined with one of the reference ionization chambers mentioned in Table 1 in the appendix. The plane parallel ionization chambers shall be covered with an additional build-up foil of sufficient thickness to achieve charged particle equilibrium.
- 2.2 *Calibration procedure:* The reference chamber (including build-up foil, when applicable) shall be calibrated in air in terms of air kerma at a Primary Standard Dosimetry Laboratory in a beam of x-rays. The quality of the calibration field shall be as close as possible to that of the user's beam.
- 2.3 *Beam quality specification:* The beam quality shall be specified by the tube voltage (kV) and first half-value layer (mm Al).
- 2.4 *Reference conditions:* The quantity to be determined is the photon absorbed dose to water at the surface of the phantom. The absorbed dose shall be determined by measurement of air kerma free-in-air (in absence of the phantom) and conversion to absorbed dose to water. The field size shall be as close as possible to 4 cm × 4 cm or 4 cm diameter at the reference distance. The reference distance is the source-surface distance normally used. The chamber (including build-up foil, when applicable) shall be placed with its reference point at the reference distance and with its geometrical centre at the central axis of the beam. The reference point of the chamber is the point to which the calibration factor applies. For measurement directly at the end of an applicator one of the plane parallel ionization chambers mentioned in Table 1 shall be used.
- 2.5 *Determination of absorbed dose to water at the reference point:* The photon absorbed dose to water at the surface of a water phantom is given by the relation:

$$D_w = M_u^{\text{free air}} N_K B_w (\bar{\mu}_{\text{en}}/\rho)_{w/\text{air}}^{\text{free air}} \quad (14)$$

where

D_w is the absorbed dose to water in the x-ray beam at the reference point when the chamber is replaced by the water phantom (phantom surface at the reference point);

$M_u^{\text{free air}}$ is the ionization chamber reading, free-in-air, corrected for:

a) any difference in ambient air conditions affecting the chamber reading at the time of

measurement compared with the standard conditions for which the calibration factor applies (temperature, pressure, humidity);

b) any difference in ion recombination and polarity effects in the user's beam compared with the calibration situation;

N_K is the air kerma calibration factor, provided by the Primary Standard Dosimetry Laboratory, which converts the ionization chamber reading for standard air conditions to air kerma for the calibration quality and geometry;

B_w is the backscatter factor (the ratio of the water kerma at the surface of a semi-infinite water phantom to the water kerma at that point in the absence of the phantom) for the reference field size and beam quality;

$(\bar{\mu}_{en}/\rho)_{w/air}^{free\ air}$ is the ratio of mass energy absorption coefficients of water and air averaged over the spectral energy fluence free-in-air.

- 2.6 *Absorbed dose at other positions in the phantom:* for relative distributions of absorbed dose (percentage depth doses or isodose curves) published data [15,16] and/or information provided by the manufacturer of the x-ray equipment shall be used.

3. Code of practice for medium energy x-rays (100-300 kV)

3.1 *Reference chamber:* The absorbed dose to water at the reference point shall be determined with the NE2571 cylindrical ionization chamber (see Table 1 in the appendix for some characteristics of this ionization chamber).

3.2 *Calibration procedure:* The reference chamber shall be calibrated in air in terms of air kerma at the Primary Standard Dosimetry Laboratory in a beam of x-rays. The quality of the calibration field shall be as close as possible to that of the user's primary beam.

3.3 *Beam quality specification:* The beam quality shall be specified by the tube voltage (kV) and first half-value layer (mm Cu or mm Al).

3.4 *Reference conditions:* The quantity to be determined is the absorbed dose to water at reference depth, d . The absorbed dose shall be determined in a water phantom at the reference depth under reference conditions.

The phantom surface shall be positioned at the source-surface distance normally used. The field size shall be 10 cm × 10 cm at the reference depth or at the surface of the phantom, whichever is normally used.

The reference depth is at 2 cm in-phantom. The geometrical centre of the reference chamber shall be placed at the reference depth and at the central axis of the beam. The chamber shall be fitted with a thin waterproof sheath.

3.5 *Determination of absorbed dose to water at the reference point:* The absorbed dose to water in a water phantom is given by the relation:

$$D_w = M_u^d N_K (\bar{\mu}_{en}/\rho)_{w/air}^d k_{ch} \quad (15)$$

where

D_w is the absorbed dose to water in the x-ray beam at the position of the geometrical centre of the chamber when the chamber is replaced by water;

M_u^d is the ionization chamber reading at reference depth, d , corrected for:

a) any difference in ambient air conditions affecting the chamber reading at the time of measurement compared with the standard conditions for which the calibration factor applies (temperature, pressure, humidity);

b) any difference in ion recombination and polarity effects in the user's beam compared with the calibration situation;

N_k is the air kerma calibration factor, provided by the Primary Standard Dosimetry Laboratory, which converts the ionization chamber reading for standard air conditions to air kerma for the calibration quality and geometry;

$(\bar{\mu}_{\text{en}}/\rho)_{\text{w,air}}^d$ is the ratio of mass energy absorption coefficients of water and air averaged over the spectral energy fluence in the water phantom at the reference depth, d ;

k_{ch} is the overall chamber correction factor.

- 3.6 *Phantom materials:* A water phantom shall be used, e.g. a cubic PMMA tank filled with water (30 cm × 30 cm × 30 cm).
- 3.7 *Absorbed dose at other positions in the phantom:* Absorbed dose at other positions in the phantom shall be obtained by performing relative measurements with a field instrument and can be related to the value determined at the reference point. For measurement of beam profiles, depth dose curves and isodose curves small ionization chambers or diamond detectors are recommended. Plane parallel ionization chambers are recommended for measurement of depth dose curves only.

4. Additional information

4.1 General comments on low and medium energy x-ray dosimetry

4.1.1 Method for measurement of first HVL

An overview of experimental techniques for HVL determination was given by Carlsson [17]. Trout *et al.* [18] made a thorough investigation of the performance of HVL measurements and applied accurate corrections for the detected scattered radiation. It was shown that a narrow beam and a sufficiently large distance between the absorber and measuring device must be used to obtain a correct HVL.

The instrument used for the attenuation measurements should have a minimal radiation quality dependence in the energy range concerned. The use of a monitor is advisable to allow for a correction for variations in output in the x-ray beam; it should be positioned in such a way that its reading is independent of the amount of absorption material placed in the beam. By limiting the field diameter the amount of scattered radiation which reaches the measuring device will be reduced, but the field dimensions must be larger than that of the sensitive volume of the measuring device. The diaphragm must be of sufficient thickness to absorb the primary beam. Care must be taken with regard to the alignment (e.g. by using a radiographic method).

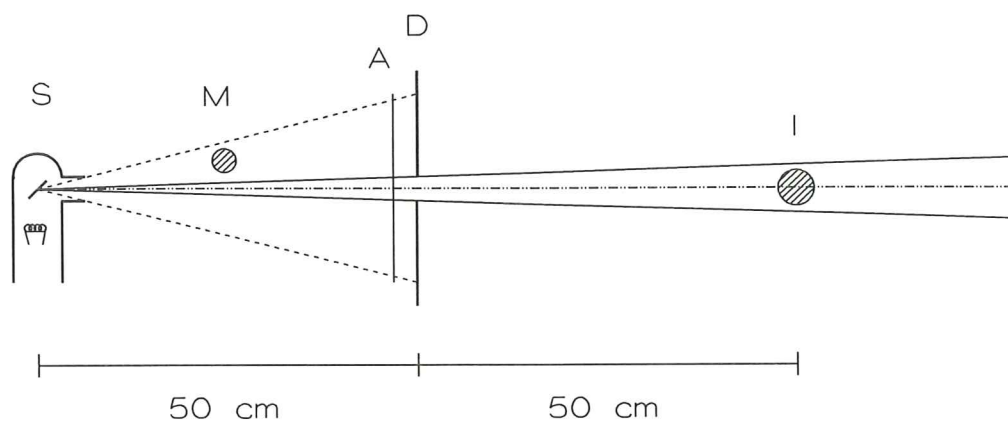


figure 1. Geometry used for HVL measurements: S, radiation source; M, monitor; A, absorber; D, diaphragm; I, ionization chamber.

An example of a simple and practical arrangement is shown in figure 1. The arrangement employs a small (e.g. 3 cm diameter) diaphragm at a distance of 50 cm from the source. Layers of the material for which the HVL is to be measured are placed on top of the diaphragm and a small detector is placed at a distance of 100 cm from the source (*i.e.* 50 cm distance from the filters).

4.1.2 Ion recombination

As the collecting potential of an ionization chamber in a radiation field is increased, the current increases until it approaches the saturation current for the given radiation intensity. The saturation current is reached if all ions formed in the sensitive volume of the chamber are collected at the electrodes. The recombination of ions decreases with increasing collecting potential. The maximum voltage applicable is limited by electron multiplication. Distinction can be made between initial and general (volume) recombination. Initial recombination can occur only between the positive and negative ions within one ionization track; it is a so-called "intratrack" process and is in practice negligible for low and medium energy x-ray dosimetry [19]. General or volume recombination occurs between ions from different ionization tracks and is a so-called "intertrack" process. General recombination is in principle dependent on the absorbed dose rate, the dimensions of the ionization chamber and the collecting potential.

The collection efficiency of ionization chambers, f , is the ratio of the measured charge, Q , to the produced charge, Q_0 :

$$f = \frac{Q}{Q_0} \quad (16)$$

For an ionization chamber exposed to continuous radiation a linear relationship between $1/f$ and $1/V^2$ was derived by Boag [19] under the condition that $f > 0.7$:

$$\frac{1}{f} = 1 + \left(\frac{\alpha}{6ek_1k_2} \right) d^4 q \left(\frac{1}{V^2} \right) \quad (17)$$

where α is the recombination coefficient, q is the charge liberated in the ionization chamber and escaping initial recombination, per unit volume and per unit of time, e is the electron charge, d is the effective electrode spacing and V is the collecting potential. The mean numerical value of the coefficient $(\alpha/6ek_1k_2)$ in air is estimated by Boag as $(6.73 \pm 0.80) \cdot 10^{13} \text{ sC}^{-1}\text{m}^{-1}\text{V}^2$. The effective electrode spacing for a cylindrical geometry can be calculated as:

$$d = (a - b) \left[\left(\frac{a + b}{a - b} \right) \frac{\ln a/b}{2} \right]^{1/2} \quad (18)$$

where a and b are the cavity radius and the radius of the inner electrode, respectively.

There exist two possibilities to derive f . Firstly, equation (17) can be solved for the specific chamber used. A second approach is to plot measured values of $1/Q$ versus $1/V^2$ and to derive Q_0 by extrapolation to infinite voltage.

4.1.3 *Absorbed dose to tissue*

In some older dosimetry protocols roentgen-to-rad conversion factors (f factors) are given to determine the absorbed dose to water or to tissue (muscle and bone), e.g. ICRU Report 17 [5]. It should be noted that, in this code of practice, recommendations are given for the determination of absorbed dose to water only. In this energy range, absorbed dose to tissue might differ significantly from absorbed dose to water.

If the differences in scattering and absorption properties of water and tissue are neglected (*i.e.* the photon fluence in water and tissue is assumed to be equal), absorbed dose to water can be converted to absorbed dose to tissue by multiplying with the mass energy absorption coefficient ratio, tissue-to-water. At this moment, a consistent set of these ratios, based on the same set of mono-energetic values of mass energy absorption coefficients and averaged over the same energy spectra applied in this code of practice, is not available.

However, in first approximation the ratios tissue-to-water of f factors can be applied to determine the dose to tissue. For muscle, this ratio varies from 0.99 for medium energy x-rays (HVL = 3.4 mm Cu) up to 1.03 for low energy x-rays (HVL = 0.7 mm Al) [20]. For bone, the variation of this ratio with photon energy is much larger.

4.2 *Comments on the code of practice for low energy x-rays*

4.2.1 *Reference chambers*

For low energy x-rays the reference ionization chamber (Table 1) is used to measure air kerma free-in-air. To prevent errors due to small differences between the spectrum of the beam used for calibration and the spectrum of the user's beam, the reference chamber should have a flat energy response.

Another important aspect is the possible difference between the field size of the beam used to calibrate the chamber and the field size of the user's beam. To avoid errors caused by differences in the field size, the response of the chamber should be independent of the field size within certain limits. At the Nederlands Meetinstituut (NMI), the response of four types of ionization chambers (NE2571, NE2611, PTW 23344 and PTW 23342) relative to the air kerma measured with a free air chamber was measured for field diameters between 2 and 10 cm. When the field diameter was decreased from 10 cm to 3 cm, the response of the PTW 23344 chamber varied about 2%. For the other chambers this variation was much less (about 1%). The NE2571 chamber can not be used for field diameters smaller than 3 cm, because its internal cavity length is 24 mm. When the field diameter was decreased from 4 cm to 2 cm, the decrease of the response was less than 2% for the PTW 23342 and

the NE2611 chambers, but more than 5% for the PTW 23344 chamber. Because of the relatively large dependence of the response of the PTW 23344 chamber on field size, it was decided not to recommend this chamber as a reference chamber.

The thickness of the thin polyethylene window of the PTW 23342 and NE2532/3 soft x-ray chambers is 2 mg cm^{-2} to 3 mg cm^{-2} . This is too thin to achieve secondary electron equilibrium, even for x-rays generated at a tube voltage of 50 kV. To act as a kerma detector, the window thickness should be at least equal to the maximum electron range. In polyethylene, $(\text{CH}_2)_n$, the electron range is about 4 mg cm^{-2} for 50 keV electrons, and 14 mg cm^{-2} for 100 keV electrons [21]. Klevenhagen *et al.* [13] showed that secondary electrons originating outside the chamber can contribute significantly to the signal, especially when there are high-Z materials present in the beam in the vicinity of the chamber, such as applicators.

Therefore, the PTW 23342 and NE2532/3 chambers should only be used as reference chambers for low energy x-rays with an additional build-up foil to achieve secondary electron equilibrium. The recommended thickness of the foil depends on the maximum electron energy and can be found in Table 2 in the appendix. The foil should also be present during calibration of the reference instrument.

The NE2561, NE2611 and NE2571 graphite cylindrical chambers have as an advantage that these chambers do not need an additional build-up foil. However, due to their shape the cylindrical chambers are not suitable for measurements directly at the end of an applicator.

4.2.2 Calibration procedure

It will be the responsibility of the Primary Standard Dosimetry Laboratory to offer a calibration at a beam quality as close as possible to that of the user's beam. Use of the reference beam qualities from Table 3 is recommended for reasons of uniformity. These beam qualities were adopted from Seelentag *et al.* [22].

In the Netherlands the Primary Standard Dosimetry Laboratory is the Nederlands Meetinstituut (NMI). In Belgium the Universiteit Gent is the acting Standards Laboratory and will be accredited by the Belgian Calibration Organization (BKO).

At NMI the standard air conditions are chosen as 22°C , 101.3 kPa and 50% relative humidity. In Belgium the standard air conditions are chosen as 20°C , 101.3 kPa and 50% relative humidity.

4.2.3 Beam quality specification

Beam quality shall be specified by the combination of peak tube voltage expressed in kilovolt and first half-value layer expressed in mm Al.

4.2.4 *Reference conditions*

For the determination of air kerma free-in-air, the field size is an important parameter because of the field size dependence of the response of the chamber. The field size dependence originates from scatter from the chamber stem. By taking the field size equal to that during calibration at the Primary Standard Dosimetry Laboratory, this scatter is accounted for in the calibration factor. Measurements made at NMI show variations of the response less than 1% for field diameters between 3 cm and 10 cm for the recommended reference chambers. For field diameters smaller than 3 cm the deviations of the response can be larger, especially for the NE2571 chamber.

4.2.5 *Determination of absorbed dose to water at the reference point*

Tables 4 and 5 in the appendix give the water kerma backscatter factor B_w as a function of first half-value layer, field diameter, and source-surface distance (SSD). The values were derived from the tables published by Grosswendt [23,24] applying linear interpolation in a linear-logarithmic plot of B_w as a function of the HVL. Also, the backscatter factors for a field diameter of 4 cm were calculated by linear interpolation in a linear-logarithmic plot of B_w as a function of the square of the field diameter. There are minor differences for small values of HVL between the values given here and those presented by the IAEA [8] which were based on earlier calculations of Grosswendt [12]. The more recent calculations are in close agreement with experimental results of Klevenhagen [25]. Measured and calculated backscatter factors were compared in a study by Carlsson [17]. The backscatter factors presented in the IPEMB code of practice [9], which were based on extensive Monte Carlo calculations performed by Knight [26], are in close agreement with those given in Table 5 (differences are smaller than 1%).

The beam qualities used by Grosswendt to calculate the backscatter factors were equal to those given in Table 3. According to Harrison [27], the use of different combinations of generating potentials and beam filters can lead to differences in the backscatter factor of up to 3% depending on the generating potential in the case of equal HVL.

It should be noted that the backscatter factors refer to a semi-infinite phantom, *i.e.* full scatter conditions apply. In a number of clinical situations, for example treatment of ear or nose, the irradiated volume has dimensions which are insufficient to give rise to full backscatter. In those cases it is necessary to apply an additional correction factor, *e.g.* those of Klevenhagen [28].

Table 6 in the appendix gives the values for the ratio of energy absorption coefficients of water and air, free-in-air, as a function of HVL [7]. The values are exclusively based on the incident primary spectra and therefore no field size or depth dependence is involved.

For some contact therapy machines, the absorbed dose rate can be very high (up to 8 Gy min^{-1}). In these cases a correction for ion recombination might be necessary. Some general information about ion recombination is given in section 4.1.2.

Additional instruments used in the absorbed dose determination, such as thermometers and barometers, should have a calibration traceable to primary standards.

4.2.6 *Absorbed dose at other positions in the phantom*

Accurate measurements of depth dose profiles and isodose curves are very difficult to achieve for low energy x-rays. The main problems are related to the energy dependence of the detector systems and the steep dose gradients, which demand a high spatial resolution of the detector system and accurate positioning. Especially in water phantoms accurate positioning can not be performed easily. Solid phantom materials are more practical but will introduce additional uncertainties due to the differences in density and elemental composition of the phantom material and water. Some information about the dependence of displacement effects on the density of the phantom material has been given by Ma and Nahum [14].

The results of a questionnaire sent to all radiotherapy centres in the Netherlands showed that it is common practice to use existing data, either provided with the x-ray machine by the manufacturer or from other sources, in most cases the data reviewed by Jennings and Harrison [15]. Recently these data were reviewed again by Harrison [16] but only minor changes were made to the PDD-tables for x-ray qualities with first HVL in the range 1.0-8.0 mm Al.

When relative absorbed dose measurements are made with one of the presently available detector systems (e.g. small ionisation chambers, diamond detectors, TLD) the uncertainties arising from the aspects mentioned above should be considered carefully. A new method based on nuclear magnetic resonance dosimetry has been presented by Kron and Pope [29].

4.3 *Comments on the code of practice for medium energy x-rays*

4.3.1 *Reference chambers*

In this code of practice only the NE2571 cylindrical chamber was selected as reference chamber for medium energy x-rays, for the following reasons:

- (1) Suitability of the chamber due to flat energy response (free-in-air) in the region of interest.
- (2) Nowadays the NE2571 is used in almost all radiotherapy institutions and centres for radiobiological research in the Netherlands and Belgium.
- (3) For the NE2571, the correction factors for different measuring depths and field diameters are well

known from Monte Carlo calculations and other methods.

4.3.2 *Calibration procedure*

It will be the responsibility of the Primary Standard Dosimetry Laboratory to offer a calibration at a beam quality as close as possible to that of the user's beam. Use of the reference beam qualities from Table 3 is recommended for reasons of uniformity. These beam qualities were also used in the International Code of Practice of the IAEA [8].

In the Netherlands the Primary Standard Dosimetry Laboratory is the Nederlands Meetinstituut (NMI). In Belgium the Universiteit Gent is the acting Standards Laboratory and will be accredited by the Belgian Calibration Organization (BKO).

At NMI the standard air conditions are chosen as 22 °C, 101.3 kPa and 50% relative humidity. In Belgium the standard air conditions are chosen as 20 °C, 101.3 kPa and 50% relative humidity.

The chamber must be calibrated without the build-up cap supplied with the chamber.

4.3.3 *Beam quality specification*

The beam quality is specified by the combination of peak tube voltage expressed in kilovolt (kV) and first half-value layer (HVL). For beams generated at tube voltages above 150 kV, HVL should be specified in mm Cu. For beams generated at tube voltages below 150 kV it is more practical to specify the HVL in mm Al. Therefore, HVL in mm Al is also given in the tables.

4.3.4 *Reference conditions*

An important difference between the present code of practice and that of the IAEA is the choice of the reference depth. In the present code of practice a reference depth of 2 cm was selected, because this depth will generally be closer to the depth of interest. As a consequence, the tables of the International Code of Practice of the IAEA can not be used directly, because these refer to a depth of 5 cm.

Table 7 gives correction factors for the influence of a PMMA waterproofing sheath. These values are based on relative measurements made at NMI with a NE2571 ionization chamber in a water phantom, fitted with PMMA sheaths with different thicknesses ranging from 2 to 25 mm. The PMMA sheath will increase the instrument reading. As can be seen from the table, the effect is more important at the lower energies.

The use of sheath materials having talcum powder, such as rubber, is not recommended, as severe

chamber response problems have been reported as a result of talcum powder entering the chamber through the venting hole [30].

4.3.5 Determination of absorbed dose to water at the reference point

Numerical values of $(\bar{\mu}_{\text{en}}/\rho)_{\text{w/air}}^{\text{d}}$ and k_{ch} are given in Tables 8 and 9. The tables refer to a depth of 2 cm in water and a field size of 10 cm × 10 cm. The values are given as a function of both first HVL and generating potential. Therefore the values of $(\bar{\mu}_{\text{en}}/\rho)_{\text{w/air}}^{\text{d}}$ and k_{ch} can be determined by interpolation to match both HVL and generating potential of a specific user's beam.

The values of $(\bar{\mu}_{\text{en}}/\rho)_{\text{w/air}}^{\text{d}}$ in Table 8 were calculated using the Monte Carlo method. Twenty five measured x-ray spectra [31], with generating potential varying between 50 kV and 250 kV, and half-value layers between 0.020 mm Cu and 4.2 mm Cu, were used as input for the calculation of the photon fluence spectra at 2 cm depth in water (field size: 10 cm × 10 cm at the phantom surface). Mass energy absorption coefficients of water and air from Hubbell [32] were averaged over the calculated photon fluence spectra at 2 cm depth, resulting in average mass energy absorption coefficient ratios at 2 cm depth for the twenty five input spectra. Finally, from these data the $(\bar{\mu}_{\text{en}}/\rho)_{\text{w/air}}^{\text{d}}$ values given in Table 8 were calculated by interpolation.

The values of the overall chamber correction factors were calculated according to the method described by Seuntjens and Verhaegen [33]. This method involves the calculation of all components of the overall chamber correction factor using the Monte-Carlo method for a range of x-ray spectra. The values of k_{ch} in Table 9 were interpolated between the values for the available x-ray spectra. According to Seuntjens and Verhaegen, the uncertainty in the overall chamber correction factors obtained with this method varies between 0.7% and 0.9%.

The results for the overall correction factor $k_{\text{a,w}}$ presented by the IAEA [7] represent an average of four different methods, namely water calorimetry [34], extrapolation chamber methods, Monte Carlo calculations, and ionization chamber measurements. The results all correspond to a depth of 5 cm. From the spread of the results obtained with the different methods the IAEA concludes that the uncertainties in the $k_{\text{a,w}}$ values have an uncertainty of 2% or 3% (one standard deviation). At this moment, no values of k_{ch} at 2 cm depth obtained with independent methods (e.g. water calorimetry) are available to validate the values in Table 9 directly. Therefore, the uncertainty in the k_{ch} values in Table 9 are assumed to be of the same order of magnitude as those presented by the IAEA. Nevertheless, the k_{ch} values are tabulated to three places of decimals to show the dependence on HVL and generating potential obtained with the Monte Carlo calculations, as well as for computational uses.

Since photon scattering contributes significantly to the spectrum at a certain depth in a phantom, both quantities $(\bar{\mu}_{\text{en}}/\rho)_{\text{w,air}}^{\text{d}}$ and k_{ch} are dependent on field size. Knight and Nahum provided $(\bar{\mu}_{\text{en}}/\rho)_{\text{w/air}}^{\text{d}}$ data

as a function of field size for a comprehensive range of therapeutic medium energy x-ray spectra [35], using similar calculational methods as described above. The results of Knight and Nahum show that, in general, $(\bar{\mu}_{en}/\rho)_{w/air}^d$ decreases with an increase in field size and the change is more significant at higher HVL. At a depth of 2 cm, a decrease of almost 2% is observed for the highest HVL considered (3 mm Cu), when the field size varies from 0 cm to 40 cm diameter. However, little variation occurs for field sizes greater than 20 cm diameter.

To estimate the variation of the overall chamber correction factor when deviating from standard field size, Seuntjens and Verhaegen [33] reanalysed each component in the definition of the overall chamber correction factor for the NE2571 ionization chamber using Monte Carlo calculations for field sizes from 20 cm² to 200 cm². The results show that the overall variations of k_{ch} with field size at 2 cm depth is less than 1% over the medium

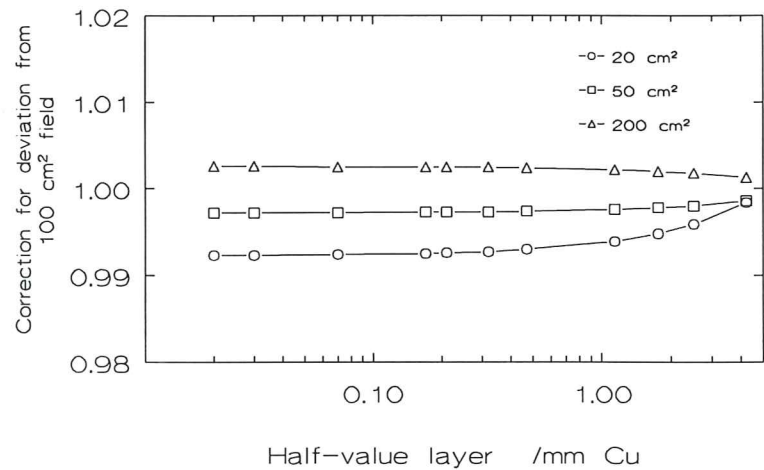


figure 2. Correction for field size dependence of k_{ch} at 2 cm depth (to be multiplied with k_{ch}).

energy x-ray range. The correction for the deviation of k_{ch} with field size (20-200 cm²) at 2 cm depth (to be multiplied with k_{ch}) is plotted in figure 2 and can be used to obtain better accuracy for non-reference field sizes.

In the present code of practice only measurements in water are recommended. However, in some cases solid phantom materials are useful. Attenuation and scatter of the primary beam as well as the overall chamber correction factor are dependent on density and elemental composition of the phantom material. The difference between the reference instrument reading in a water phantom and, for instance, a polystyrene phantom can be up to a few percent. The reading observed in such a phantom should be converted to absorbed dose to water. The conversion procedure will introduce additional uncertainties. Some information about the dependence of displacement effects on the density of the phantom material has been given by Ma and Nahum [14].

By using a vertical beam, no correction for the PMMA walls of the water phantom has to be applied.

Additional instruments used in the absorbed dose determination, such as thermometers and barometers, should have a calibration traceable to primary standards.

4.3.6 Absorbed dose at other positions in the phantom

As pointed out in section 4.2.6, accurate measurements of depth dose profiles and isodose curves for low energy x-rays are difficult to achieve for several reasons. The same reasons also apply to medium energy x-rays, but generally the corrections and uncertainties are smaller in the medium energy range.

The results of a questionnaire sent to all radiotherapy centres in the Netherlands show that it is common practice to use existing data, either provided with the x-ray machine by the manufacturer or from other sources, in most cases the data reviewed by Jennings and Harrison [15] for x-ray qualities with HVL smaller than 0.5 mm Cu, and by Smith and Sutherland [36] for x-ray qualities with HVL larger than 0.5 mm Cu. Some radiotherapy centres perform measurements as a check, in most cases by using a small ionisation chamber in a water phantom. Methods for such measurements in the medium energy region are described by Scrimger and Connors [37], Niroomand-Rad *et al.* [38] and Gerig *et al.* [39]. The results presented by these and other authors have been reviewed recently by Smith [40].

The formalism presented in this code of practice is in principle also valid at depths in the phantom other than the reference depth. However, since photon scattering contributes significantly to the spectrum at a certain depth in a phantom, both quantities $(\bar{\mu}_{\text{en}}/\rho)_{\text{w,air}}^{\text{d}}$ and k_{ch} are not only dependent on field size, but also on depth in the phantom. Knight and Nahum provided $(\bar{\mu}_{\text{en}}/\rho)_{\text{w,air}}^{\text{d}}$ data as a function of depth for a comprehensive range of therapeutic medium energy x-ray spectra [35]. For a fixed field size of 10 cm diameter, Knight and Nahum observe a variation of $(\bar{\mu}_{\text{en}}/\rho)_{\text{w,air}}^{\text{d}}$ with depth of approximately 0.5% within the first 5 cm for higher HVLs (HVL greater than 1 mm Cu). For lower HVLs, no clear trends can be distinguished.

Seuntjens and Verhaegen [33] calculated the overall chamber correction factor for the NE2571 ionization chamber at 2 cm and 5 cm depth using Monte Carlo methods. For medium energy x-rays, they concluded that, when the depth increases from 2 cm to 5 cm, the variation of k_{ch} is negligible (*i.e.* smaller than about 1%).

In some codes of practice the concept of effective point of measurement is used, to correct for displacement effects when an ionization chamber is used for measurements in a phantom. However, in this code of practice, the overall chamber correction factor corrects for all effects including displacement effects. For measurements at the reference depth, the ionization chamber should be placed with its geometrical centre at the reference point. Although the displacement effect is in principle depth dependent, this dependence will generally be small for small ionization chambers. Seuntjens and Verhaegen [33] found that the variation of this effect was less than 0.5 % for a Farmer size cavity between 2 cm and 5 cm depth for radiation qualities in the medium-energy x-ray range.

4.4 *Detectors to be used for relative dosimetry of low and medium energy x-rays*

Accurate measurements of relative depth dose curves for low and medium energy x-rays are complicated due to the large gradients of the dose distribution in phantoms and the extreme energy dependence of most of the practical detector systems used for relative dosimetry. Cylindrical ionization chambers are not suitable to measure absorbed dose close to the surface. For other detectors, such as photographic film and TLD, their energy dependence may prevent them from being suitable to measure kerma in the phantom. Diode detectors (shielded or unshielded) are not suitable for relative dosimetry of low and/or medium energy x-rays because their energy response changes by a factor of 2 or 4 over the energy range of interest. As a general rule, the variation of the air-kerma response of a given detector (*e.g.* an electron parallel plate ionization chamber or a diamond detector) must be established in order to estimate their accuracy for relative dosimetry purposes and their range of applicability.

In a separate study, the suitability of diamond detectors to measure depth kerma curves for relative dosimetry of medium energy x-rays was investigated [41]. Relative depth dose curves measured with a diamond were compared with measurements with a well characterized NE2571 ionization chamber at depths greater than 2 cm. The result of this comparison showed that for the radiation qualities classified as medium energy in this code, the diamond detector can be used for relative dosimetry of medium energy x-rays without energy correction. The dose value at 10 cm depth measured with the NE2571 ionization chamber and the diamond detector agree to within 8%. For lower energies (down to 80 kV, HVL: 2.6 mm Al), the maximum deviations amount to 12% of the absorbed dose value. Correction factors are provided for the diamond detectors to account for the energy dependence of their response as a function of depth from 0.2 cm to 10 cm in case a higher accuracy is desired.

5. References

1. NCS (Netherlands Commission on Radiation Dosimetry), Code of practice for the dosimetry of high-energy photon beams, NCS Report 2, NCS, Delft (1986)
2. NCS (Netherlands Commission on Radiation Dosimetry), Code of practice for the dosimetry of high-energy electron beams, NCS Report 5, NCS, Delft (1989).
3. NCS (Netherlands Commission on Radiation Dosimetry), Recommendations for the dosimetry and quality control of radioactive sources used in brachytherapy, NCS Report 4, NCS, Delft (1991).
4. NCS (Netherlands Commission on Radiation Dosimetry), Dosimetric Aspects of Mammography, NCS Report 6, NCS, Delft (1993).
5. ICRU (International Commission on Radiation Units and Measurements), Radiation Dosimetry: X Rays Generated at Potentials of 5 to 150 kV, ICRU Report 17, ICRU, Washington, D.C. (1970).
6. ICRU (International Commission on Radiation Units and Measurements), Measurement of Absorbed Dose in a Phantom Irradiated by a Single Beam of X or Gamma Rays, ICRU Report 23, ICRU, Washington, D.C. (1973).
7. IAEA (International Atomic Energy Agency), Review of data and methods recommended in the international code of practice IAEA Technical Reports Series No. 227, Absorbed Dose Determination in Photon and Electron Beams, Proceedings of a consultants meeting, Vienna, 8-11 December 1992, IAEA-TECDOC-897, IAEA, Vienna (1996).
8. IAEA (International Atomic Energy Agency), Absorbed Dose Determination in Photon and Electron Beams: An International Code of Practice, Technical Report Series No. 277, IAEA, Vienna (1987).
9. IPEMB (Institution of Physics and Engineering in Medicine and Biology), The IPEMB code of practice for the determination of absorbed dose for x-rays below 300 kV generating potential (0.035 mm Al-4 mm Cu HVL, 10-300 kV generating potential), Phys. Med. Biol. 41, 2605-2625 (1996).
10. MA, C.-M. and NAHUM, A.E., Bragg-Gray theory and ion chamber dosimetry in photon beams, Phys. Med. Biol. 36, 413-428 (1991).
11. NAHUM, A.E. and KNIGHT, R.T., Consistent formalism for kilovoltage X ray dosimetry, Measurement Assurance in Dosimetry (Proc. Symp. Vienna, 1993), pp 451-459, IAEA, Vienna (1994).
12. GROSSWENDT, B., Backscatter factors for x-rays generated at voltages between 10 and 100 kV, Phys. Med. Biol. 29, 579-591 (1984).
13. KLEVENHAGEN, S.C., D'SOUZA, D. and BONNEFOUX, I., Complications in low energy x-ray dosimetry caused by electron contamination, Phys. Med. Biol. 36, 1111-1116 (1991).
14. MA, C.-M. and NAHUM, A.E., Calculations of ion chamber displacement effect corrections for medium-energy x-ray dosimetry, Phys. Med. Biol. 40, 45-62 (1995).
15. JENNINGS, W.A. and HARRISON, R.M., X Rays: HVL range 0.01 to 8.0 mm Al, in Central Axis Depth Dose Data for Use in Radiotherapy, Br. J. Radiol. (Supplement 17), The British Institute of Radiology, London (1983).

16. HARRISON, R.M., X Rays: Half-value layers 0.01 to 8.0 mm Al (approx. 6-150 kV peak potential difference), *in* Central Axis Depth Dose Data for Use in Radiotherapy: 1996, Br. J. Radiol. (Supplement 25), The British Institute of Radiology, London (1996).
17. CARLSSON, C.A., Differences in reported backscatter factors for low-energy x-rays: a literature study, *Phys. Med. Biol.* 38, 521-531 (1993).
18. TROUT, E.D., KELLY, J.P. and LUCAS, A.C., Determination of Half-Value Layer, *Am. J. Roentgenol.* 84, 729-740 (1960).
19. BOAG, J.W., Ionization chambers, *in* Radiation Dosimetry (K.R. Kase, B.E. Bjärngård and F.H. Attix, eds.), Vol. 2, pp. 169-243, Academic Press, New York (1987).
20. JAEGER, S.S. and HARNISCH, B.D., and Reply by WYCKOFF, H.O., Corrected f factors for photons from 10 keV to 2 MeV, *Communications, Med. Phys.* 10, 715-717 (1983).
21. ICRU (International Commission on Radiation Units and Measurements), Stopping Powers for Electrons and Positrons, ICRU Report 37, ICRU, Bethesda, MD. (1973).
22. SEELENTAG, W.W., PANZER, W., DREXLER, G., PLATZ, L. and SANTNER, F., A catalogue of spectra for the calibration of dosimeters, GSF Report 560, Gesellschaft für Strahlen- und Umweltforschung, München (1979).
23. GROSSWENDT, B., Dependence of the photon backscatter factor for water on source-to-phantom distance and irradiation field size, *Phys. Med. Biol.* 35, 1233-1245 (1990).
24. GROSSWENDT, B., Dependence of the photon backscatter factor for water on irradiation field size and source-to-phantom distances between 1.5 and 10 cm, *Phys. Med. Biol.* 38, 305-310 (1993).
25. KLEVENHAGEN, S.C., Experimentally determined backscatter factors for x-rays generated at voltages between 16 and 140 keV, *Phys. Med. Biol.* 34, 1871-1882 (1989).
26. KNIGHT, R.T., Backscatter Factors for Low- and Medium-energy x-rays calculated by the Monte Carlo Method, Internal Report ICR-PHYS-1/93, Royal Marsden NHS Trust, Sutton, Surrey, (1993).
27. HARRISON, R.M., Backscatter factors for diagnostic radiology, *Phys. Med. Biol.* 27, 1465-1474 (1982).
28. KLEVENHAGEN, S.C., The build-up of backscatter in the energy range 1 mm Al to 8 mm Al, *Phys. Med. Biol.* 27, 1035-1043 (1982).
29. KRON, T. and POPE, J.M., Dose distribution measurements in superficial x-ray beams using NMR dosimetry, *Phys. Med. Biol.* 39, 1337-1349 (1994).
30. HANSON, W.F., ARNOLD, D.J., SHALEK, R.J. and HUMPHRIES, L.J., Contamination of ionization chambers by talcum powder, *Med. Phys.* 15, 776-777 (1983).
31. SEUNTJENS, J., THIERENS, H., VAN DER PLAETSEN, A. and SEGAERT, O., Conversion factor f for x-ray beam qualities, specified by peak tube potential and HVL value, *Phys. Med. Biol.* 32, 595-603 (1987).
32. HUBBELL, J.H., Photon mass attenuation and energy-absorption coefficients from 1 keV to 20 MeV, *Int. J. Appl. Radiat. Isot.* 33, 1269-1290 (1982).

33. SEUNTJENS, J. and VERHAEGEN, F., Dependence of overall correction factor of a cylindrical ionization chamber on field size and depth in medium-energy x-ray beams, *Med. Phys.* 23, 1789-1796 (1996).
34. SEUNTJENS, J., THIERENS, H. and SCHNEIDER, U., Correction factors for cylindrical ionisation chambers used in medium energy x-ray beams, *Phys. Med. Biol.* 38, 805-832 (1993).
35. KNIGHT, R.T. and NAHUM, A.E., Depth and field-size dependence of ratios of mass energy absorption coefficient, water to air, for kilovoltage x ray dosimetry, *Measurement Assurance in Dosimetry (Proc. Symp. Vienna, 1993)*, pp 361-370, IAEA, Vienna (1994).
36. SMITH, C.W. and SUTHERLAND, W.H., X Rays: hVL range 0.5 to 4.0 mm Cu, *in Central Axis Depth Dose Data for Use in Radiotherapy*, Br. J. Radiol. (Supplement 17), The British Institute of Radiology, London (1983).
37. SCRIMGER, J.W. and CONNORS, S.G., Performance characteristics of a widely used orthovoltage x-ray unit, *Med. Phys.* 13, 267-269 (1986).
38. NIROOMAND-RAD, A., GILLIN, M.T., LOPEZ, F. and GRIMM, D.F., Performance characteristics of an orthovoltage x-ray therapy machine, *Med. Phys.* 14, 874-878 (1987).
39. GERIG, L., SOUBRA, M. and SALHANI, D., Beam characteristics of the Therapax DXT300 orthovoltage therapy unit, *Phys. Med. Biol.* 39, 1377-1392 (1994).
40. SMITH, C.W., Orthovoltage X-ray beams (0.5 mm-4.0 mm Cu hVL), *in Central Axis Depth Dose Data for Use in Radiotherapy: 1996*, Br. J. Radiol. (Supplement 25), The British Institute of Radiology, London (1996).
41. SEUNTJENS, J., AALBERS, A.H.L., GRIMBERGEN, T.W.M., MIJNHEER, B.J., THIERENS, H., VAN DAM, J., WITTKAMPER, F.W., ZOETELIEF, J., PIESSENS, M. and PIRET, P., On the use of diamond detectors to measure central axis depth kerma curves for low and medium energy x-rays, draft (1997).

APPENDIX: Numerical values

Table 1. Characteristics of reference ionization chambers for low energy x-rays. For medium energy x-rays, only the NE2571 chamber is recommended as reference chamber.

| Chamber type | Chamber geometry | Volume (cm ³) | Wall material | Wall thickness (mg cm ⁻²) | Manufacturer |
|--------------|------------------|---------------------------|-----------------|---------------------------------------|------------------|
| 23342 | plane parallel | 0.02 | CH ₂ | 2.5 | PTW ¹ |
| 2532/3 | plane parallel | 0.03 | CH ₂ | 2-3 | NE ² |
| 2561 | cylindrical | 0.325 | graphite | 90 | NE ² |
| 2611 | cylindrical | 0.325 | graphite | 90 | NE ² |
| 2571 | cylindrical | 0.6 | graphite | 65 | NE ² |

¹PTW: PTW-Freiburg GmbH, Freiburg, Germany

²NE: Bicron-NE Ltd, Beenham, Reading, United Kingdom

Table 2. Required thickness of additional polyethylene build-up foil for reference ionization chambers with a 2.5 mg cm⁻² polyethylene window. The maximum range is the range in polyethylene according to the continuous-slowing-down-approximation (CSDA) [21], for secondary electrons with maximum kinetic energy for a given generating potential. The last column gives approximate values for the thickness of the foil in μm for practical use.

| Generating potential (kV) | Maximum range (mg.cm ⁻²) | Thickness of additional build-up foil | |
|------------------------------|---|---------------------------------------|-------------------|
| | | (mg.cm ⁻²) | (μm) |
| 50 | 4.025 | 1.5 | 20 |
| 60 | 5.541 | 3.0 | 30 |
| 70 | 7.249 | 4.7 | 50 |
| 80 | 9.134 | 6.6 | 70 |
| 90 | 11.18 | 8.7 | 95 |
| 100 | 13.39 | 10.9 | 120 |

Table 3. Reference beam qualities for low and medium energy x-rays [22].

| Generating potential (kV) | Added filtration | 1st HVL (mm Al) | 1st HVL (mm Cu) |
|---------------------------|------------------|-----------------|-----------------|
| 50 | 1.05 mm Al | 1.04 | |
| 50 | 4.05 mm Al | 2.24 | |
| 70 | 3.6 mm Al | 2.94 | |
| 100 | 3.5 mm Al | 4.28 | 0.17 |
| 120 | 6.0 mm Al | 6.31 | 0.30 |
| 140 | 9.0 mm Al | 8.45 | 0.49 |
| 150 | 0.5 mm Cu | | 0.83 |
| 200 | 1.15 mm Cu | | 1.70 |
| 250 | 1.6 mm Cu | | 2.47 |
| 280 | 3.0 mm Cu | | 3.37 |

Notes: Not included in the added filtration are the inherent filtration of the tube, and the air path. For the qualities with generating potential up to 150 kV, the inherent filtration was 3 mm Be and the air path 75 cm. For the qualities with generating potential higher than 150 kV, the inherent filtration was 2.4 mm Al equivalent and the air path 225 cm.

For a specific x-ray unit, HVL values may differ from the values given in the table due to the effects of target angle, anode roughening, inherent filtration, voltage ripple and air absorption.

Table 4. Kerma-based backscatter factor for a water phantom for SSD between 1.5 and 7 cm. Values are derived from Grosswendt [24].

| SSD (cm) | Field diameter (cm) | 1st HVL (mm Al) | | | | | | | | | | | | |
|-------------|---------------------------|-----------------|-------|-------|-------|-------|-------|-------|-------|-------|-------|-------|-------|-------|
| | | 0.10 | 0.15 | 0.2 | 0.3 | 0.4 | 0.5 | 0.6 | 0.8 | 1.0 | 1.5 | 2 | 3 | 4 |
| 1.5 | 1 | 1.015 | 1.019 | 1.023 | 1.028 | 1.032 | 1.036 | 1.038 | 1.042 | 1.045 | 1.051 | 1.055 | 1.057 | 1.057 |
| | 2 | 1.018 | 1.025 | 1.031 | 1.039 | 1.046 | 1.052 | 1.057 | 1.065 | 1.070 | 1.082 | 1.091 | 1.097 | 1.098 |
| | 3 | 1.018 | 1.026 | 1.033 | 1.042 | 1.049 | 1.056 | 1.063 | 1.072 | 1.079 | 1.094 | 1.105 | 1.114 | 1.116 |
| | 4 | 1.018 | 1.026 | 1.033 | 1.043 | 1.050 | 1.058 | 1.064 | 1.074 | 1.082 | 1.098 | 1.110 | 1.120 | 1.122 |
| | 5 | 1.018 | 1.026 | 1.033 | 1.043 | 1.050 | 1.058 | 1.065 | 1.076 | 1.085 | 1.102 | 1.114 | 1.125 | 1.128 |
| | 10 | 1.018 | 1.027 | 1.034 | 1.043 | 1.051 | 1.059 | 1.066 | 1.077 | 1.086 | 1.104 | 1.117 | 1.129 | 1.132 |
| 3 | 15 | 1.018 | 1.027 | 1.034 | 1.043 | 1.051 | 1.059 | 1.066 | 1.077 | 1.086 | 1.104 | 1.117 | 1.129 | 1.133 |
| | 20 | 1.018 | 1.027 | 1.034 | 1.043 | 1.051 | 1.059 | 1.066 | 1.077 | 1.086 | 1.104 | 1.117 | 1.129 | 1.133 |
| | 1 | 1.015 | 1.019 | 1.023 | 1.028 | 1.032 | 1.036 | 1.039 | 1.043 | 1.046 | 1.051 | 1.055 | 1.060 | 1.058 |
| | 2 | 1.018 | 1.026 | 1.033 | 1.043 | 1.050 | 1.057 | 1.062 | 1.071 | 1.078 | 1.092 | 1.102 | 1.111 | 1.110 |
| | 3 | 1.018 | 1.028 | 1.036 | 1.048 | 1.056 | 1.065 | 1.073 | 1.084 | 1.093 | 1.113 | 1.127 | 1.140 | 1.142 |
| | 4 | 1.019 | 1.029 | 1.037 | 1.049 | 1.059 | 1.069 | 1.077 | 1.090 | 1.101 | 1.124 | 1.140 | 1.157 | 1.160 |
| 5 | 5 | 1.019 | 1.029 | 1.038 | 1.051 | 1.061 | 1.071 | 1.079 | 1.094 | 1.107 | 1.132 | 1.150 | 1.170 | 1.175 |
| | 10 | 1.019 | 1.030 | 1.039 | 1.052 | 1.062 | 1.073 | 1.083 | 1.099 | 1.113 | 1.141 | 1.162 | 1.188 | 1.195 |
| | 15 | 1.019 | 1.030 | 1.039 | 1.052 | 1.062 | 1.073 | 1.083 | 1.099 | 1.114 | 1.142 | 1.163 | 1.191 | 1.198 |
| | 20 | 1.019 | 1.030 | 1.039 | 1.052 | 1.062 | 1.073 | 1.083 | 1.099 | 1.114 | 1.143 | 1.164 | 1.192 | 1.199 |
| | 1 | 1.014 | 1.020 | 1.023 | 1.029 | 1.033 | 1.037 | 1.039 | 1.043 | 1.046 | 1.052 | 1.056 | 1.060 | 1.058 |
| | 2 | 1.019 | 1.027 | 1.034 | 1.044 | 1.051 | 1.058 | 1.065 | 1.074 | 1.081 | 1.095 | 1.105 | 1.115 | 1.113 |
| 7 | 3 | 1.019 | 1.030 | 1.038 | 1.050 | 1.059 | 1.069 | 1.077 | 1.089 | 1.098 | 1.119 | 1.134 | 1.150 | 1.152 |
| | 4 | 1.019 | 1.030 | 1.039 | 1.052 | 1.062 | 1.073 | 1.083 | 1.097 | 1.109 | 1.134 | 1.152 | 1.173 | 1.178 |
| | 5 | 1.019 | 1.031 | 1.040 | 1.054 | 1.064 | 1.077 | 1.087 | 1.103 | 1.117 | 1.145 | 1.166 | 1.191 | 1.198 |
| | 10 | 1.019 | 1.031 | 1.041 | 1.055 | 1.067 | 1.081 | 1.093 | 1.112 | 1.129 | 1.165 | 1.190 | 1.228 | 1.241 |
| | 15 | 1.019 | 1.031 | 1.041 | 1.055 | 1.067 | 1.081 | 1.093 | 1.113 | 1.131 | 1.168 | 1.195 | 1.235 | 1.250 |
| | 20 | 1.019 | 1.031 | 1.041 | 1.055 | 1.067 | 1.081 | 1.093 | 1.113 | 1.131 | 1.168 | 1.195 | 1.237 | 1.252 |
| 7 | 1 | 1.014 | 1.020 | 1.023 | 1.029 | 1.033 | 1.036 | 1.039 | 1.043 | 1.046 | 1.052 | 1.056 | 1.061 | 1.060 |
| | 2 | 1.018 | 1.028 | 1.035 | 1.045 | 1.053 | 1.060 | 1.066 | 1.075 | 1.083 | 1.097 | 1.107 | 1.119 | 1.118 |
| | 3 | 1.019 | 1.030 | 1.039 | 1.051 | 1.061 | 1.070 | 1.078 | 1.091 | 1.101 | 1.123 | 1.139 | 1.157 | 1.157 |
| | 4 | 1.019 | 1.031 | 1.040 | 1.054 | 1.064 | 1.075 | 1.084 | 1.100 | 1.114 | 1.141 | 1.160 | 1.185 | 1.188 |
| | 5 | 1.019 | 1.031 | 1.041 | 1.055 | 1.066 | 1.079 | 1.089 | 1.107 | 1.123 | 1.154 | 1.176 | 1.207 | 1.213 |
| | 10 | 1.019 | 1.032 | 1.043 | 1.058 | 1.070 | 1.084 | 1.096 | 1.118 | 1.139 | 1.181 | 1.210 | 1.256 | 1.271 |
| 15 | 15 | 1.019 | 1.032 | 1.043 | 1.058 | 1.070 | 1.085 | 1.096 | 1.120 | 1.142 | 1.187 | 1.219 | 1.269 | 1.288 |
| | 20 | 1.019 | 1.032 | 1.043 | 1.058 | 1.070 | 1.085 | 1.096 | 1.120 | 1.143 | 1.188 | 1.220 | 1.272 | 1.293 |

Table 5. Kerma-based backscatter factor for a water phantom for SSD between 10 and 100 cm. Values are derived from Grosswendt [23].

| SSD (cm) | Field diameter (cm) | 1st HVL (mm Al) | | | | | | | | | | |
|-------------|---------------------------|-----------------|-------|-------|-------|-------|-------|-------|-------|-------|-------|-------|
| | | 0.10 | 0.15 | 0.2 | 0.3 | 0.4 | 0.5 | 0.6 | 0.8 | 1.0 | 1.5 | 2 |
| 10 | 1 | 1.014 | 1.020 | 1.024 | 1.030 | 1.034 | 1.037 | 1.039 | 1.043 | 1.046 | 1.052 | 1.056 |
| | 2 | 1.019 | 1.028 | 1.035 | 1.044 | 1.052 | 1.059 | 1.066 | 1.075 | 1.083 | 1.096 | 1.106 |
| | 3 | 1.019 | 1.029 | 1.038 | 1.051 | 1.061 | 1.071 | 1.079 | 1.093 | 1.103 | 1.123 | 1.137 |
| | 4 | 1.019 | 1.031 | 1.041 | 1.054 | 1.065 | 1.077 | 1.087 | 1.103 | 1.117 | 1.143 | 1.162 |
| | 5 | 1.019 | 1.032 | 1.042 | 1.057 | 1.069 | 1.082 | 1.093 | 1.111 | 1.126 | 1.158 | 1.180 |
| | 10 | 1.019 | 1.033 | 1.044 | 1.060 | 1.074 | 1.090 | 1.103 | 1.126 | 1.147 | 1.190 | 1.221 |
| 20 | 1 | 1.019 | 1.033 | 1.044 | 1.060 | 1.074 | 1.091 | 1.105 | 1.129 | 1.151 | 1.198 | 1.231 |
| | 2 | 1.019 | 1.033 | 1.044 | 1.061 | 1.075 | 1.092 | 1.106 | 1.131 | 1.153 | 1.200 | 1.233 |
| | 3 | 1.014 | 1.020 | 1.024 | 1.030 | 1.034 | 1.037 | 1.040 | 1.044 | 1.047 | 1.053 | 1.058 |
| | 4 | 1.018 | 1.028 | 1.035 | 1.046 | 1.054 | 1.061 | 1.066 | 1.076 | 1.084 | 1.098 | 1.108 |
| | 5 | 1.020 | 1.031 | 1.040 | 1.052 | 1.062 | 1.071 | 1.079 | 1.093 | 1.105 | 1.126 | 1.140 |
| | 10 | 1.020 | 1.034 | 1.045 | 1.062 | 1.076 | 1.092 | 1.105 | 1.131 | 1.156 | 1.205 | 1.240 |
| 30 | 1 | 1.020 | 1.034 | 1.046 | 1.063 | 1.077 | 1.094 | 1.108 | 1.135 | 1.163 | 1.218 | 1.258 |
| | 2 | 1.020 | 1.034 | 1.046 | 1.063 | 1.077 | 1.095 | 1.109 | 1.138 | 1.166 | 1.223 | 1.263 |
| | 3 | 1.015 | 1.020 | 1.024 | 1.028 | 1.032 | 1.036 | 1.038 | 1.043 | 1.047 | 1.054 | 1.059 |
| | 4 | 1.018 | 1.028 | 1.035 | 1.045 | 1.053 | 1.060 | 1.065 | 1.075 | 1.084 | 1.099 | 1.109 |
| | 5 | 1.019 | 1.030 | 1.039 | 1.052 | 1.062 | 1.071 | 1.079 | 1.094 | 1.108 | 1.128 | 1.142 |
| | 10 | 1.020 | 1.034 | 1.045 | 1.062 | 1.076 | 1.092 | 1.105 | 1.131 | 1.158 | 1.207 | 1.243 |
| 50 | 1 | 1.020 | 1.034 | 1.046 | 1.063 | 1.077 | 1.095 | 1.109 | 1.138 | 1.166 | 1.222 | 1.262 |
| | 2 | 1.020 | 1.034 | 1.046 | 1.063 | 1.077 | 1.095 | 1.110 | 1.140 | 1.170 | 1.229 | 1.271 |
| | 3 | 1.014 | 1.020 | 1.023 | 1.029 | 1.033 | 1.036 | 1.039 | 1.042 | 1.045 | 1.052 | 1.058 |
| | 4 | 1.018 | 1.028 | 1.035 | 1.046 | 1.054 | 1.060 | 1.065 | 1.074 | 1.082 | 1.097 | 1.109 |
| | 5 | 1.019 | 1.031 | 1.040 | 1.053 | 1.063 | 1.072 | 1.080 | 1.094 | 1.106 | 1.128 | 1.144 |
| | 10 | 1.019 | 1.033 | 1.045 | 1.062 | 1.077 | 1.095 | 1.109 | 1.136 | 1.160 | 1.212 | 1.249 |
| 100 | 1 | 1.019 | 1.033 | 1.046 | 1.063 | 1.078 | 1.097 | 1.113 | 1.142 | 1.170 | 1.229 | 1.271 |
| | 2 | 1.019 | 1.033 | 1.046 | 1.063 | 1.078 | 1.098 | 1.114 | 1.144 | 1.174 | 1.235 | 1.279 |
| | 3 | 1.014 | 1.020 | 1.024 | 1.030 | 1.034 | 1.037 | 1.039 | 1.042 | 1.044 | 1.051 | 1.057 |
| | 4 | 1.018 | 1.028 | 1.035 | 1.046 | 1.054 | 1.060 | 1.065 | 1.073 | 1.080 | 1.097 | 1.109 |
| | 5 | 1.019 | 1.031 | 1.040 | 1.054 | 1.063 | 1.072 | 1.080 | 1.092 | 1.104 | 1.128 | 1.144 |
| | 10 | 1.019 | 1.033 | 1.046 | 1.063 | 1.078 | 1.095 | 1.109 | 1.135 | 1.159 | 1.212 | 1.250 |

Table 6. Ratio of mass energy absorption coefficients of water and air, free-in-air, for low energy x-rays as a function of first half-value layer [7].

| 1st HVL (mm Al) | $(\bar{\mu}_{en}/\rho)_{w/air}^{free\ air}$ |
|--------------------|---|
| 0.10 | 1.048 |
| 0.15 | 1.045 |
| 0.2 | 1.041 |
| 0.3 | 1.036 |
| 0.4 | 1.033 |
| 0.5 | 1.030 |
| 0.6 | 1.027 |
| 0.8 | 1.024 |
| 1.0 | 1.021 |
| 1.5 | 1.018 |
| 2 | 1.017 |
| 3 | 1.023 |
| 4 | 1.028 |

Table 7. Correction factors (to be multiplied with the ionization chamber reading) for measurements in a water phantom with a NE2571 ionization chamber surrounded by a PMMA sheath as a function of its thickness (see text paragraph 4.3.4 for details).

| First HVL | | Thickness PMMA sheath (mm) | | |
|-----------|---------|----------------------------|-------|-------|
| (mm Cu) | (mm Al) | 1 | 3 | 5 |
| 0.10 | 2.8 | 0.997 | 0.990 | 0.983 |
| 0.15 | 3.7 | 0.997 | 0.991 | 0.985 |
| 0.2 | 4.4 | 0.997 | 0.992 | 0.986 |
| 0.3 | 6.1 | 0.997 | 0.993 | 0.988 |
| 0.4 | 7.8 | 0.998 | 0.994 | 0.990 |
| 0.5 | 9.1 | 0.998 | 0.995 | 0.992 |
| 0.6 | | 0.998 | 0.996 | 0.993 |
| 0.8 | | 0.998 | 0.996 | 0.994 |
| 1.0 | | 0.999 | 0.997 | 0.995 |
| 1.5 | | 0.999 | 0.998 | 0.996 |
| 2 | | 1.000 | 0.999 | 0.998 |
| 3 | | 1.000 | 1.000 | 0.999 |
| 4 | | 1.000 | 1.000 | 1.000 |
| 5 | | 1.000 | 1.000 | 1.000 |

Table 8. Ratio of mass energy absorption coefficients of water and air at 2 cm depth in water and for field size 10 cm × 10 cm, as a function of first HVL (in mm Cu or mm Al) and generating potential (see text paragraph 4.3.5 for details).

| First HVL | | Generating potential (kV) | | | | | | |
|-----------|---------|---------------------------|-------|-------|-------|-------|-------|-------|
| (mm Cu) | (mm Al) | 100 | 120 | 140 | 150 | 200 | 250 | 280 |
| 0.10 | 2.8 | 1.025 | 1.030 | | | | | |
| 0.15 | 3.7 | 1.026 | 1.032 | | | | | |
| 0.2 | 4.4 | 1.028 | 1.033 | 1.037 | | | | |
| 0.3 | 6.1 | 1.031 | 1.036 | 1.040 | 1.042 | | | |
| 0.4 | 7.8 | 1.034 | 1.039 | 1.043 | 1.045 | | | |
| 0.5 | 9.1 | | 1.042 | 1.046 | 1.048 | | | |
| 0.6 | | | | 1.049 | 1.051 | | | |
| 0.8 | | | | | 1.058 | | | |
| 1.0 | | | | | 1.062 | 1.063 | | |
| 1.5 | | | | | 1.072 | 1.073 | | |
| 2 | | | | | | 1.080 | 1.084 | |
| 3 | | | | | | 1.093 | 1.093 | 1.093 |
| 4 | | | | | | | 1.103 | 1.103 |
| 5 | | | | | | | 1.112 | 1.112 |

Table 9. Overall chamber correction factor, k_{ch} , for the NE2571 cylindrical ionization chamber at 2 cm depth in water and for field size 10 cm × 10 cm, as a function of first HVL (in mm Cu or mm Al) and generating potential (see text paragraph 4.3.5 for details).

| First HVL | | Generating potential (kV) | | | | | | |
|-----------|---------|---------------------------|-------|-------|-------|-------|-------|-------|
| (mm Cu) | (mm Al) | 100 | 120 | 140 | 150 | 200 | 250 | 280 |
| 0.10 | 2.8 | 1.008 | 1.011 | | | | | |
| 0.15 | 3.7 | 1.014 | 1.017 | | | | | |
| 0.2 | 4.4 | 1.018 | 1.020 | 1.022 | | | | |
| 0.3 | 6.1 | 1.020 | 1.021 | 1.023 | 1.024 | | | |
| 0.4 | 7.8 | 1.021 | 1.022 | 1.024 | 1.024 | | | |
| 0.5 | 9.1 | | 1.023 | 1.024 | 1.024 | | | |
| 0.6 | | | | 1.024 | 1.024 | | | |
| 0.8 | | | | | 1.024 | | | |
| 1.0 | | | | | 1.024 | 1.023 | | |
| 1.5 | | | | | 1.023 | 1.018 | | |
| 2 | | | | | | 1.015 | 1.015 | |
| 3 | | | | | | 1.010 | 1.010 | 1.010 |
| 4 | | | | | | | 1.004 | 1.004 |
| 5 | | | | | | | 1.001 | 1.001 |

Publications of the Netherlands Commission on Radiation Dosimetry

| | |
|---|-------|
| <i>Radiation dosimetry activities in the Netherlands.</i> Inventory compiled under the auspices of the Netherlands Commission for Radiation Dosimetry. NCS Report 1, July 1986. | n.a. |
| <i>Code of practice for the dosimetry of high-energy photon beams.</i> NCS Report 2, December 1986. | f20,- |
| <i>Proceedings of the Symposium on Thermoluminescence Dosimetry.</i> NCS Report 3, October 1988. | f20,- |
| <i>Aanbevelingen voor dosimetrie en kwaliteitscontrole van radioactieve bronnen bij brachytherapie.</i> NCS Report 4, Februari 1989 (in Dutch). | |
| <i>Recommendations for dosimetry and quality control of radioactive sources used in brachytherapy.</i> Synopsis (in English) of NCS Report 4, February 1991. | f20,- |
| <i>Code of practice for the dosimetry of high-energy electron beams.</i> NCS Report 5, December 1989. | f20,- |
| <i>Dosimetric aspects of Mammography.</i> NCS Report 6, March 1993. | f25,- |
| <i>Recommendations for the calibration of Iridium-192 high dose rate sources.</i> NCS Report 7, December 1994. | f25,- |
| <i>Kwaliteitscontrole van Medische Lineaire Versnellers, methoden voor kwaliteitscontrole, wenselijke toleranties en frequenties.</i> NCS Report 8, December 1995 (in Dutch). | f25,- |
| <i>Quality Control of Medical Linear Accelerators, current practice and minimum requirements.</i> NCS Report 9, August 1996. | f25,- |
| <i>Dosimetry of low and medium energy x-rays, a code of practice for use in radiotherapy and radiobiology.</i> NCS Report 10, July 1997. | f25,- |

From within The Netherlands reports can be ordered by paying the amount into ABN-AMRO account nr. 51.70.64.332 to the credit of "Nederlandse Commissie voor Stralingsdosimetrie", stating the report number(s). Please add f5,- for postage and packing.

From outside The Netherlands, please complete the order form below.

| ORDER FORM | | |
|---|--|----------------|
| Please send this completed order form to: NCS secretary, P.O.Box 654, 2600 AR DELFT, The Netherlands | | |
| QTY | REPORT TITLE | COST |
| | | |
| | | |
| | | |
| | | |
| | | Subtotal |
| Add postage and packing (Europe f10,-, outside Europe f20,-) | | |
| | | Total |
| Payment by: | <input type="checkbox"/> Cheque/postal order* made payable to Netherlands Commission on Radiation Dosimetry (add f15,- for banking costs) | |
| | <input type="checkbox"/> Please charge my Eurocard/Mastercard | |
| | Credit card No. | |
| | Expiry date | |
| Name: | | |
| Address: | | |
| | | |
| Date: | Signature: | |
| | | |
| * please delete as applicable | | NCS report 10 |